# Advanced glycation end products modulate amyloidogenic APP processing and Tau phosphorylation: a mechanistic link between glycation and the development of Alzheimer's disease

Kedar Batkulwar[a,b], Rashmi Godbole[a], Reema Banarjee[a,b], Omar Kassaar[c], Robert J Williams[c]*, Mahesh J Kulkarni[a,b]*

[a]Proteomics Facility, Division of Biochemical Sciences, CSIR-National Chemical Laboratory, Pune-411008, India.

[b]Academy of Scientific and Innovative Research (AcSIR), CSIR-National Chemical Laboratory, Pune-411008, India.

[c]Department of Biology and Biochemistry, University of Bath, Bath, BA2 7AY, UK.

*For correspondence

1. Mahesh J Kulkarni, PhD

Scientist, Proteomics Facility

Division of Biochemical Sciences

CSIR-National Chemical Laboratory

Pune-411008, India

E-mail: mj.kulkarni@ncl.res.in

2. Robert J Williams, PhD

Department of Biology and Biochemistry

University of Bath

Bath-BA2 7AY, UK

E-mail: R.J.Williams@bath.ac.uk

## ABSTRACT

Advanced glycation end products (AGEs) are implicated in the pathology of Alzheimer's disease (AD), as they induce neurodegeneration following interaction with the receptor for AGE (RAGE). This study aimed to establish a mechanistic link between AGE-RAGE signaling and AD pathology. AGE-induced changes in the neuro2a proteome were monitored by SWATH-MS. Western blotting and cell-based reporter assays were used to investigate AGE-RAGE regulated APP processing and tau phosphorylation in primary cortical neurons. Selected protein expression was validated in brain samples affected by AD. AGE-RAGE axis altered proteome included increased expression of Cathepsin B and asparagine endopeptidase (AEP), which mediated increase in $A\beta_{1-42}$ formation and tau phosphorylation, respectively. Elevated Cathepsin B, AEP, RAGE, and pTau levels were found in human AD brain coincident with enhanced AGEs. This study demonstrates that AGE-RAGE axis regulates $A\beta_{1-42}$ formation and tau phosphorylation via increased Cathepsin B and AEP, providing a new molecular link between AGEs and AD pathology.


**KEYWORDS:** Advanced glycation end products, Alzheimer's disease, Amyloid beta, Asparagine endopeptidase, Cathepsin B, Diabetes, Proteomics, Tau phosphorylation.

## INTRODUCTION

Alzheimer's disease (AD) is a one of the major causes of dementia in older people leading to cognitive dysfunction.[1] AD is characterized by accumulation of insoluble extracellular senile plaques and intracellular neurofibrillary tangles.[2, 3] The disease affects over 47 million people worldwide and this number is expected to increase to more than 131 million by 2050 as per the World Alzheimer Report 2016. AD is a multifactorial syndrome involving several molecular and cellular processes including inflammation, mitochondrial dysfunction, glycation, protein aggregation, oxidative stress and hyperglycemia.[4-8]

The occurrence of AD is significantly higher in an aging population, as well as in subjects with diabetes, suggesting that dysregulation in glucose metabolism could be one of the causal factors.[9, 10] The peptide hormone insulin has been directly implicated in tau hyperphosphorylation via activation of ERK and GSK3β. Thus hyperinsulinemia is associated with neurofibrillary tangles formation and hence AD progression. In contrast, insulin is also known to promote processing of APP through a non-amyloidogenic pathway, and insulin resistance is associated with increased deposition of Aβ and reduced brain function.[10-13] The inevitable consequence of increased insulin resistance is hyperglycemia leading to protein glycation. Glycation is a non-enzymatic reaction between glucose or other glycolysis intermediates and proteins leading to formation of heterogeneous advanced glycation end products (AGEs).[14] The levels of AGEs increase during biological aging due to decreased efficiency of homeostatic processes.[15] AGEs are associated with AD pathology and are likely involved in the formation of amyloid plaques and neurofibrillary tangles.[7, 16-18] AGEs can induce toxic effects through interactions with the cell surface AGE receptor (RAGE). AD brain shows increased RAGE expression which is involved in the intraneuronal transport of Aβ peptides leading to mitochondrial damage and neuronal dysfunction.[19, 20] Furthermore, glycated Aβ has been shown to exacerbate neuronal damage, through interaction with RAGE, as it acts as a more suitable ligand over unmodified Aβ.[21] Blocking RAGE

signaling with the inhibitor, FPS-ZM1, was found to be effective in reducing Aβ-mediated neuronal dysfunction in an AD mouse model highlighting the potential importance of AGE-RAGE in AD pathology and progression.[22] The precise mechanisms involved are not fully defined but RAGE stimulation leads to activation of NADPH oxidases which induces reactive oxygen species (ROS) generation. Redox imbalance induces activation of several signal transduction pathways which damage cells and tissues severely.[23]

Thus, the aim of the current study was to explore the change in the neuronal protein profile in response to AGE-RAGE signaling and investigate the role of selected regulated proteins in the development of AD pathology. Human serum albumin (HSA) is the predominant AGE modified protein in plasma, and AD individuals show increased glycated proteins in Cerebrospinal fluid.[24, 25] Using AGE-HSA as a ligand for RAGE, we performed label-free quantitative proteomic analysis by SWATH-MS, showing that AGE/RAGE axis regulates several key proteins implicated in AD including Cathepsin B, asparagines endopeptidase (AEP), acid ceramidase and CD147. The AGE/RAGE axis stimulated an increase in Cathepsin B-mediated APP processing, which was associated with increased $A\beta_{1-42}$ formation in primary cortical neurons. AGE/RAGE interaction also led to increased tau phosphorylation. Further, we have observed increased levels of RAGE, Cathepsin B and AEP correlating with higher levels of AGE modified proteins and phosphorylated tau in brain homogenates from the temporal cortex of individuals affected by AD. Hence this study describes a direct association between the AGE/RAGE axis and the development of AD providing a new mechanistic link between AGEs and dementia.

## RESULTS

### Synthesis of AGE-HSA

AGE-HSA was synthesized by co-incubating glucose and HSA for 90 days under sterile conditions. Formation of AGEs was confirmed by measuring AGE-specific fluorescence and western blotting with anti-carboxymethyllysine (CML) antibody as showed in Figure S2 (Supplementary). Furthermore, AGE-

HSA was thoroughly characterised for AGE modifications using high resolution accurate mass spectrometry (Supplementary methods). A list of modified peptides is provided in Supplemental Table S1.

**AGE-HSA induces ROS and apoptosis in neuro2a cells**

AGE-RAGE axis activates NADPH oxidase and stimulates reactive oxygen species (ROS) production[26], which further activates NF-κB leading to inflammation and apoptosis.[27] Therefore, to investigate the role of AGE-RAGE axis, we have studied the effects of AGE-HSA on cell viability, ROS production and apoptosis. Cell viability was assessed by 3-(4,5-dimethylthiazol-2-yl)-2,5-diphenyltetrazolium bromide (MTT) dye reduction assay, an indicator of metabolic status. AGE-HSA was significantly cytotoxic to neuro2a cells at a concentration of 1.5 mg/ml and above (Figure 1) compared to unmodified HSA, which was used as a control. Lower concentration of AGE-HSA (0.1, 0.5 and 1 mg/ml) however, did not show any cytotoxic effects (Figure 1). Therefore, AGE-HSA at a non-cytotoxic concentration of 1 mg/ml was chosen to conduct all subsequent experiments. Next, the influence of AGE-HSA on ROS production was studied by 2′,7′-Dichlorofluorescin diacetate (DCF-DA) staining. ROS induced formation of fluorescent 2′, 7′-dichlorofluorescein was monitored by fluorescent spectrometry. HSA and AGE-HSA stimulation showed 1.08 and 1.35 fold increase in the levels of ROS respectively as compared to control (Figure 2A). Images acquired using fluorescence microscope also showed increase in the DCF-DA fluorescence in AGE-HSA stimulated cells (Figure 2B). Furthermore, AGE-HSA induced apoptosis was studied using Annexin V-FITC staining followed by flow cytometry. Cells treated with AGE-HSA showed 7 % apoptotic cells, which is about 2 fold higher than unmodified HSA (Figure 2 C-E).

**AGE-HSA regulates expression of key proteins involved in AD**

Proteomic analysis (SWATH-MS) was performed to better understand the effect of AGE-HSA on neuronal cells. A spectral library created from tryptic peptides of control and AGE-HSA treated cells comprised of 1610 proteins (Supplemental Table S2). SWATH analysis revealed expression of 35 up

regulated (>2 fold) and 36 down regulated (<2 fold) proteins upon AGE-HSA induction compared to HSA (Supplemental Table S3). Functional annotation by DAVID analysis suggested that the differentially expressed proteins were involved in diverse biological processes as shown in Figure 3A and 3B. Briefly, up regulated proteins were involved in fatty acid metabolism, proteolysis, lipid metabolism and redox processes (Supplemental Table S4), while down regulated proteins were involved in mRNA processing, protein synthesis and transport and cell adhesion. Furthermore, the differentially expressed proteins were subjected to iRegulon analysis, a cytoscape plugin for prediction of transcription factors which probably regulate these proteins. It showed that the up regulated proteins might be co-regulated by transcription factors such as Nfyb, Hsf2 and Gfi1b (Figure 3C), while down regulated proteins might be co-regulated by transcription factors such as Etv4 and E2f1 (Figure 3D). Protein-protein interaction network analysis revealed interactions of differentially regulated proteins and were found to be involved mainly in the lysosomal degradation pathway (Figure 3E). The most notable findings from the proteomic analysis was the up regulation of number of lysosomal proteins; Cathepsin B (4.83, p=0.04), asparagine endopeptidase (AEP)/legumain (4.71, p=0.00003) and acid ceramidase (5.40, p=0.003) and the down regulation of CD147 (0.46, p=0.02), as these proteins have been directly implicated in AD (Figure 3F).

**AGE-HSA regulates the expression of Cathepsin B and AEP in mouse primary cultured cortical neurons through RAGE**

Exposure to AGEs caused 184.51% and 546.87% increase in the expression of Cathepsin B and AEP respectively in neuro2a cells confirming the initial proteomic analysis (Figure 4A, 4B and 4C). As Cathepsin B and AEP are directly involved in Aβ formation and tau hyperphosphorylation respectively[28, 29], we also studied the AGE-RAGE-dependent expression of these two proteins in primary cortical neurons, which is a better model system for investigating the regulation of these proteins. The expression of RAGE was confirmed in primary cortical neurons by western blotting (Figure S3, supplementary) and AGE-HSA was not toxic at 1.0 mg/ml as shown by MTT assay (Figure S4, supplementary). Expression of Cathepsin B and AEP following exposure to AGEs was studied by Western blotting. As predicted,

Cathepsin B and AEP expression was elevated by 154.78% and 208.64% respectively in response to AGEs. Significantly, blocking RAGE with an anti-RAGE antibody (H300) abolished AGE-induced Cathepsin B and AEP expression demonstrating that up regulation requires an AGE-RAGE interaction (Figure 4D, 4E and 4F).

**AGE-RAGE interaction increases Cathepsin B-dependent APP processing, β-CTF formation and Aβ generation**

Cathepsin B is a well-characterized lysosomal cysteine protease in mammalian cells which plays an important role in intracellular proteolysis.[30] It selectively cleaves APP at the Beta-secretase 1 (BACE1) site[31] and is associated with the accumulation of $A\beta_{1-40}$ and $A\beta_{1-42}$. Furthermore, the Cathepsin B inhibitor, CA074Me, reduces brain Aβ deposition and improves memory deficits in AD animal models by inhibiting Cathepsin B.[31] Transgenic mice lacking the Cathepsin B gene displayed reduced Aβ deposition.[32, 33] All these studies suggest an important role for Cathepsin B in APP processing and AD pathology. AGEs increase BACE1 expression [34] but effects on Cathepsin B are much less clear. Hence, we studied the sensitivity of APP processing to a selective Cathepsin B inhibitor, CA074Me using an APP-GAL4 luciferase reporter assay in primary cortical neurons which preferentially reports amyloidogenic βγ-secretase dependent processing. [35, 36] Exposure to AGE-HSA, but not HSA alone, led to a robust increase in luciferase expression that was sensitive to the γ-secretase inhibitor N-[N-(3,5-Diflurophenaacetyl-L-alanyl)]-S-phenylglycine t-Butyl Ester (DAPT)suggesting that AGEs couple to an amyloidogenic APP processing pathway in neurons (Figure 5A). Notably the AGEs-induced increase in luciferase expression was reversed in the presence of Cathepsin B inhibitor CA074Me suggesting that AGE-HSA induced increases in APP processing was mediated primarily by Cathepsin B (Figure 5B). Furthermore, the anti-RAGE antibody H300 also strongly inhibited APP processing, indicating that AGEs increase APP processing via association with RAGE (Figure 5B). Cathepsin B gene knockout mice have substantially reduced levels of the C-terminal β-secretase fragment (β-CTF) derived from APP processing,[32] hence APP-CTFs were measured after exposure of neurons to AGE-HSA (Figure 5C).

AGE-HSA treatment appeared to increase β-CTF formation compared with control or HSA alone, as seen as a diffuse band around 10 kDa by Tris-tricine SDS-PAGE followed by Western blot with anti-APP-CTF antibody. Treatment with the Cathepsin B inhibitor CA074Me or the anti-RAGE antibody H300, decreased β-CTF formation suggesting that Cathepsin B regulated β-CTF formation is downstream of activation of the AGE-RAGE axis. Elevated β-CTF levels in neurons could equally be mediated by β-secretase; therefore, the effect of the BACE1 inhibitor, AZD3293 on AGEs-mediated β-CTF formation was also investigated. AZD3293 also reduced β-CTF formation and appeared to switch processing to the formation of α-CTFs as seen as a diffuse lower molecular weight band. Collectively, these findings suggest that both Cathepsin B and β-secretase contribute to AGE-mediated β-CTF formation. Furthermore, in order to determine if activation of the AGE-RAGE axis resulted in Aβ formation we also quantified $A\beta_{1-42}$ levels by ELISA in the growth media of AGE-HSA treated primary cortical neurons. Exposure of primary cortical neurons to AGE-HSA resulted in a ~two-fold increase in the secretion of $A\beta_{1-42}$ compared with HSA alone and a ~3-fold increase in $A\beta_{1-42}$ compared with non-treated control (Figure 5D). The AGEs-induced increase in $A\beta_{1-42}$was reduced by treatment with either CA074Me or H300 consistent with our hypothesis that AGEs couple to amyloidogenic APP processing through recruitment of the AGE-RAGE axis and subsequent activation of Cathepsin B. AZD3293 also reduced AGE-induced $A\beta_{1-42}$ secretion but this was likely due to a strong inhibitory effect on basal $A\beta_{1-42}$ levels in the absence of AGEs which is in general agreement with previous reports that the favoured constitutive APP processing route in primary neurons is via BACE.

**AGE-HSA induces tau phosphorylation**

Our initial proteome measurements demonstrated that AGEs up regulate the expression of AEP in neurons. Previous studies have implicated AEP in hyperphosphorylation of tau via activation of inhibitor of protein phosphatase 2A (PP2A) involved in dephosphorylation of tau[28, 37] and the AGE-RAGE axis activates various kinases including Akt, ERKs, GSK3β,[38] which are also involved in hyperphosphorylation of tau. Therefore, we assessed the tau phosphorylation status in response to AGE-

HSA treatment in primary cortical neurons. Neither HSA nor AGE-HSA altered the levels of tau (Figure 6), but enhanced tau phosphorylation, as evidenced by elevated phosphorylation at Serine396 after AGE-HSA stimulation. However, the increase in pTau S396 observed with AGE-HSA was not restored following co-incubation with an anti-RAGE antibody (H300) (Figure 6) suggesting a mechanism of regulation independent of RAGE

**Validation of AGE, RAGE, Cathepsin B, AEP and phosphorylation of tau in the AD brain**

CML, a predominant AGE modification[39] was analyzed in human tissue homogenates prepared from the temporal cortex of AD and control brains. A representative western blot of 6 subjects, 3 each of healthy age matched control and AD patients are showed in Figure 7A. Quantification of western blot revealed that there was 1.35 fold increase ($p$=0.1486) in CML modification of proteins in the brain lysate of AD patients as compared to healthy subjects (Figure 7B). Further accumulation of AGEs is associated with elevated RAGE expression.[40] As expected, AD brain showed 1.31 fold ($p$=0.1290) increase in levels of RAGE expression as compared to age matched controls (Figure 7C). Cathepsin B and AEP expression were also markedly increased by 1.82 ($p$=0.0957) and 1.56 ($p$=0.0268) fold respectively in the human AD brain (Figure 7D and 7E) supporting the proteome and functional data obtained in cell models. The elevated expression of AEP was also reflected with increased tau phosphorylation (2.51 fold, $p$=0.1202) in AD subjects. Further, levels of RAGE, Cathepsin B, AEP, pTau and CML modified proteins in Normal and AD subjects was normalized with beta-tubulin which revealed significant increase in their levels across the groups (Table 1). To our knowledge, this is the first study that reports increased expression of Cathepsin B and AEP in AD brain.

**Discussion**

The RAGE is a multi-ligand transmembrane receptor which interacts with various ligands including advanced glycation end products (AGEs), HMGB, S100, and Aβ. Long-lived proteins are preferentially glycated to form AGEs, which interact with RAGE and exacerbate neurodegeneration.[41] The proteasomal

system is impaired during aging leading to accumulation of modified proteins including AGEs. Furthermore, protein glycation is increased in the Cerebrospinal fluid of individuals with AD as compared with age-matched controls.[24, 42, 43] Glycated Aβ is hypothesized as a more suitable ligand for RAGE[21] and high levels of AGEs are associated with poorer learning in AD mice.[44] Several studies show RAGE dependent increase in ROS generation which further activates nuclear factor (NF)-κB.[27] NF-κB plays an important role in transducing inflammatory and pro-apoptotic signals.[45] RAGE-dependent activation of NF-κB leads to the up-regulation of RAGE itself.[46] Noticeable increase in RAGE levels and oxidative damage is observed in the brain of AD subjects suggesting vital role of ROS in the development AD.[8, 47] Despite decades of evidences that shows AGEs accumulate during AD, influence Aβ toxicity and clearance, and drive changes through redox actions,[48, 49] the precise molecular mechanisms linking AGEs to the development and progression of AD pathology are still not well understood. In this study we have investigated the change in proteome in response to AGE treatment in neuro2a cells using label free quantitative approach (SWATH-MS) to discover new proteins and pathways that lead to AD progression downstream of the AGE-RAGE axis. A number of key lysosomal proteins previously implicated in AD, including Cathepsin B, asparagine endopeptidase (AEP) and acid ceramidase, were up regulated by AGEs. Activation of the AGE-RAGE axis in neurons stimulated Cathepsin B-mediated APP processing and increased $A\beta_{1-42}$ formation. Furthermore, AGE-RAGE signaling increased expression of AEP and tau phosphorylation.

Cathepsin B, a cysteine protease, is involved in APP processing through its BACE1 activity leading to elevated Aβ formation. Inhibitors of Cathepsin B, CA074Me and E64d, have been shown to improve memory function by reducing Aβ levels in transgenic mice overexpressing wild type APP.[29, 31] The improvement in memory was also demonstrated by Cathepsin B gene knock out in transgenic mice overexpressing wild type APP.[32, 33] In our study also we have demonstrated AGE-HSA induced upregulation of Cathepsin B in neuro2a, primary cortical neurons, and in brain tissue from individuals with AD subjects. Interestingly, higher levels of Cathepsin B have previously been reported in the plasma of AD subjects.[50] The increased expression of Cathepsin B was also associated with enhanced

amyloidogenic APP processing, β-CTF and $A\beta_{1-42}$ formation all of which were reduced in the presence of a Cathepsin B inhibitor or by H300 an anti-RAGE antibody. Collectively, this study suggests that Cathepsin B may have a potential role in aggravating the onset and development of $A\beta_{1-42}$ pathology in sporadic AD particularly in association with type II diabetes where elevated levels of AGEs may induce up regulation of Cathepsin B expression.

Neurofibrillary tangles, the second major pathological hallmark of AD are characterized by tau hyperphosphorylation. The deregulation of protein kinases and/or protein phosphatases is probably the primary cause of elevated tau phosphorylation.[51] Several protein kinases including members of the MAPK family, GSK-3β, cyclin-dependent kinase 5 (cdk5), can phosphorylate tau and are regulated by AGE/RAGE axis.[52-54] Methylglyoxal induced AGEs are linked with tau hyperphosphorylation through GSK-3β and p38 MAPK activation.[55] Protein phosphatase 2A (PP2A) is predominantly associated with the dephosphorylation of tau. *In vivo* PP2A activity is regulated by a protein called inhibitor-2 ($I_2^{PP2A}$). The $I_2^{PP2A}$ is cleaved by asparagine endopeptidase (AEP) into active fragments, N-terminal ($I_{2NTF}$) and C-terminal ($I_{2CTF}$), which binds to PP2A leading to its inactivation.[37] Hence, elevated expression of AEP is associated with decreased PP2A activity leading to tau hyperphosphorylation highlighting its potential role in AD pathology.[28] In this study, we demonstrated AGE-HSA induced up regulation of AEP in neuro2a and primary cortical neurons. AEP levels were found to be elevated in brain tissue of AD subjects. The increased expression of AEP was also associated with increased tau phosphorylation which was notrestored by pre-treatment with anti-RAGE antibody suggesting a RAGE independent regulation. AEP plays a critical role in tau-related clinical and neuropathological changes during aging which degrades tau, terminate its microtubule assembly function, induces tau aggregation and triggers neurodegeneration. Hence, inhibition of AEP is a potential therapeutic approach to treat tau-mediated neurodegenerative diseases.[56]

## CONCLUSION

In summary, using label free quantitative proteomics approach (SWATH-MS), a total of 1196 proteins were identified from murine neuro2a cells after HSA and AGE-HSA stimulation. AGE induced differential expression of 71 proteins, of which 35 were up regulated and 36 down regulated. Differentially regulated proteins included Cathepsin B, AEP, acid ceramidase and CD147, all of which have been implicated in AD pathology. Furthermore, AGE-RAGE induced Cathepsin B mediated increase in $A\beta_{1-42}$ formation was observed highlighting the importance of AGE/RAGE axis in APP processing. In addition to actions on Aβ pathology, an AGE-RAGE induced increase in tau phosphorylation was also established, perhaps via increased expression and activity of AEP. Individuals affected by AD showed notable increase in the expression of Cathepsin B and AEP signifying their potential deregulation in AD. This study for the first time demonstrates that AGEs regulate both $A\beta_{1-42}$ generation and tau phosphorylation, the two key hallmarks of AD, following increased expression of lysosomal proteases, thus providing a direct molecular link between the accumulation of AGEs and the development of AD pathology in sporadic disease and particularly in association with diabetes and hyperglycemia.

## METHODS

### Antibodies

Cathepsin B was detected using rabbit anti-cathespin B antibody (Santa Cruz Biotechnology (SCBT), #sc-6493-R). Asparagine endopeptidase (AEP) was detected using rabbit anti-AEP antibody (Abcam, #ab125286). RAGE was detected by using rabbit anti-RAGE antibody (SCBT, #H-300). APP and APP-CTFs were detected using monoclonal rabbit anti-APP C-terminal antibody (Abcam, #ab32136). Tau was detected using mouse monoclonal anti-tau46 antibody (Cell Signaling Technology (CST), #4019). Tau phosphosite-specific westerns were performed using the mouse monoclonal anti-pS396/PHF13 (CST, #9632) and anti-pSer202, pThr205/AT8 (Thermo scientific, #MN1020) antibodies. Carboxymethylation

of proteins was detected using rabbit anti-CML (Abcam, #ab27684) antibody. Anti-Tubulin Antibody, beta III isoform (Millipore, #MAB1637) was used as a routine loading control. Anti-mouse (Millipore, AP124P) and anti-rabbit (Millipore, AP132P) peroxidase conjugated secondary antibodies were used to detect primary antibodies.

**Cell culture**

Neuro2a cells were purchased from National Centre for Cell Science, Pune, India. Cells were cultured in DMEM (Himedia, #AL183A) supplemented with10% heat-inactivated fetal bovine serum (Himedia, #RM9955) at 37°C in 5% $CO_2$.[57] The presence of RAGE in neuro2a cells was confirmed by Western blotting (Figure S1, Supplementary). Primary cortical neurons were prepared from CD1 mouse embryos in accordance with UK Home Office Guidelines as stated in the Animals (Scientific Procedures) Act 1986 using Schedule 1 procedures approved by the University of Bath Animal Welfare and Ethical Review Body. Primary neurons were prepared essentially as described previously.[58] Cortices were dissected from 15-day-old CD1 mouse embryos, and were mechanically dissociated in PBS ($Ca^{2+}$ and $Mg^{2+}$ free) supplemented with 6mM glucose, using a serum coated fire-polished glass Pasteur pipette. Cells were plated into either 12- or 24-well Nunc tissue culture plates, previously coated with 20 μg/ml poly-D-lysine (Sigma). Neurons were cultured in neurobasal medium (Life Technologies, #12348017), supplemented with 2 mM glutamine, 100 μg/ml penicillin, 60 μg/ml streptomycin and B27 (Life Technologies, #10889038) and incubated at 37°C, in high humidity with 5% $CO_2$. Under these growth conditions at 5-10 days *in vitro* (DIV) cells had a well-developed neuritic network and were 99% β-tubulin III positive and <1% GFAP positive.

**3-(4,5-dimethylthiazol-2-yl)-2,5-diphenyltetrazolium bromide (MTT) dye reduction assay for cell viability**

The effect of AGEs on cell viability was determined by MTT assay. Neuro2a cells or primary cortical neurons were incubated with various concentrations of HSA or AGE-HSA (0.1, 0.5, 1, 1.5 mg/ml) for 24

h and MTT (2.4 mM) (Sigma, #M5655) was then added for a further3 h at 37°C in a 5% $CO_2$ incubator. After incubation, the culture media was removed by aspiration and formazan crystals were dissolved in 100% DMSO. The absorbance was measured at 550 nm using Bio-Rad iMark microplate reader.[59]

**Measurement of intracellular ROS**

ROS was detected by 2′, 7′-dichlorofluorescin diacetate (Sigma, #D6883) staining followed by plate-based measurement of fluorescence and imaging. As the process of NADPH oxidase activation and ROS generation is an instantaneous process via adaptor molecules, ROS measurement was performed after 1h of AGE treatment. Cells were treated with HSA or AGE-HSA for 1 h at 37°C. After wash with PBS, the cells were stained with DCF-DA (10 μM) for 10 min at 37°C and fluorescence intensity was read using a fluorescence microplate reader (Thermo Scientific Varioskan Flash) at 485/528 nm excitation/emission wavelengths respectively.[60, 61] Further, fluorescent images were captured by microscopy (Life technologies, Evos).

**Apoptosis assay**

AGE induced apoptosis was studied using an Annexin V-FITC apoptosis detection kit (Sigma, #APOAF).[62, 63] Cells were treated with HSA or AGE-HSA for 24 h and stained with propidium iodide (PI) and Annexin V-FITC for 10 min. Carboplatin (10 μM) or methylglyoxal (3 mM) was applied to cells to induce either apoptosis or necrosis respectively, followed by PI or Annexin V-FITC Staining. PI and FITC fluorescence was measured using an Accuri Flow Cytometer (BD Biosciences) as per the manufacturer's instructions. Data analysis was performed using BD Accuri C6 software and the percentage of apoptotic cells was determined.

**Sample preparation for Mass spectrometric analysis**

Neuro2a cells were treated with HSA or AGE-HSA (1 mg/ml) for 24 h. Protein extraction was performed in 50 mM ammonium bicarbonate buffer containing 0.1% Rapigest SF (Waters, #186001860) followed

by 30 min incubation on ice with intermittent mixing. Protein concentration was determined using a Bio-Rad Bradford assay kit. 100 µg of protein was used for digestion. Proteins were denatured by heating at 80°C for 15 min. Further, proteins were reduced and alkylated by 100 mM dithiothreitol at 60°C for 15 min and 200 mM iodoacetamide at room temperature for 30 min respectively. 4 µg of proteomics grade porcine trypsin (Sigma, # T6567) was added and incubated for 18 h at 37°C. Samples were acidified with formic acid to stop the digestion; tryptic peptides were desalted by using C18 zip-tips (Millipore, #ZTC18S096) and concentrated using vacuum concentrator.[64] Peptides were reconstituted in 3% ACN with 0.1% formic acid before being subjected to LC-MS/MS analysis.

**Liquid chromatography-mass spectrometry analysis (SWATH-MS)**

All samples were analyzed on an AB Sciex Triple-TOF 5600 mass spectrometer coupled with micro LC 200 (Eksigent) in high-sensitivity mode. To generate the SWATH spectral library, peptide digests of each treatment were analyzed by LC-MS/MS in an Information Dependent Acquisition (IDA) mode. All raw mass spectrometry data files have been deposited to the PeptideAtlas with the data set identifier PASS01086. A spectral library was created by combining the files of all the treatments. Accumulation time for MS and MS/MS was set to 0.25 ms and 0.01 ms respectively and fragmentation was undertaken using rolling collision energy. MS scans were performed in the mass range of 350-1800 m/z, with a charge state 2 to 5 and MS/MS was triggered for ions exceeding 120 cps.[65]

SWATH-MS datasets were acquired (in biological duplicates and technical triplicates) on micro LC-Triple TOF 5600.The desalted tryptic peptides were injected onto a Eksigent C18-RP HPLC column (100 × 0.3 mm, 3 µm, 120 Å) at the flow rate of 8 µL/min over 120 min gradient conditions, solvent A (water with 0.1 % formic acid) and solvent B (ACN with 0.1 % formic acid): held at 97 % A for 5 min, 97-90 % A over 20 min, 90-70 % A over 70 min, 70-50 % A over 5 min, 50-10 % A over 1 min, at 10 % A for 7 min, 10-97% A over 1 min and held at 97 % A for 11 min. For SWATH-MS data acquisition, the instrument was tuned to optimize the quadrupole settings for the precursor ion selection window of 25 Da

wide using 34 windows of 25 Da effective isolation width (with an additional 1 Da overlap) and with a dwell time of 70 ms to cover the mass range of 350-1200 m/z in 3.4 s. Before each cycle, an MS1 scan was acquired, and then the MS2 scan cycle started (350–375 m/z precursor isolation window for the first scan, 374–400 m/z for the second scan 1174–1200 m/z for the last scan). The collision energy for each window was set using the collision energy of a $2^+$ ion centered in the middle of the window with a spread of 15 eV.[66]

**Protein Identification and Quantification**

To obtain spectral library from IDA runs, data was analyzed by Protein Pilot software 5.0 (1% FDR) using UniProt *Mus musculus* database containing more than 16500 reviewed protein entries (2015). Validation was performed through a false discovery rate set to 1% at protein. Specificity of trypsin digestion was set for cleavage after lysine or arginine. The precursor and fragment initial mass error tolerance was set to 0.05 Da and 0.1 Da respectively. Spectral library was used as database for the analysis of SWATH data with MS and MS/MS mass error of 20 ppm and 30 ppm respectively. SWATH files were exported to Marker View which gives quantitative analysis of proteins, peptides and ions in different samples.[65]

**Experimental Design and Statistical Rationale**

The data set contains mass spectrometry results from the analysis of 2 biological and 3 technical replicates of neuro2a cell samples leading to 12 raw files considered for statistical analysis. For each analyzed sample, the values of the technical replicates were averaged and subjected to the statistical analysis. The proteins with a minimum 2-fold change (normalized with total intensity) and p values under 0.05 were considered significantly regulated.

**DAVID and Cytoscape analysis**

*Mus musculus* uniprot accessions of differentially expressed proteins were uploaded to functional annotation tool DAVID and functional clustering and pathway enrichment was performed with high stringency.[67] Further, differentially regulated proteins were analysed using the iRegulon plugin of Cytoscape 3.3 to determine proteins under common regulator.[68] The dysregulated proteins were further analysed for protein-protein interactions using String and closely interacting proteins were identified using MCL algorithm of Clustermaker2 plugin in Cytoscape.[69]

**Western blotting**

Neuro2a cells or primary cortical neurons were harvested in RIPA buffer (150 mM NaCl, 1 mM EDTA, 1% Triton X-100, 0.5% deoxycholic acid, 50 mM Tris–HCl, pH 7.5), kept on ice with intermittent mixing and centrifuged at 4°C. 10 µg of protein lysate was separated on 10% SDS-PAGE, transferred onto polyvinylidene difluoride (Millipore, #ISEQ10100) membrane and incubated for 1 h at room temperature in blocking buffer containing 3% BSA dissolved in PBST (NaCl 136.89 mM, KCl 2.68 mM, $Na_2HPO_4$ 10.14 mM and 0.1% Tween 20). The membranes were incubated overnight at 4°C with primary antibody in blocking buffer. The following antibodies were used, anti-Cathepsin B (1:500), anti-AEP (1:1000), anti-RAGE (1:500), anti-tau (1:1000), Anti-pS396Tau (1:1000), AT8 (1:1000) and anti-CML (1:2000). The membranes were incubated either with anti-rabbit or anti-mouse HRP conjugated secondary antibody at a dilution of 1:2500 for 60 min at room temperature. Immunodetection was performed using the Amersham ECL prime (GE Healthcare, RPN2232) western blotting detection reagent following the manufacturer's instructions.

**Detection of APP695 and APP C-terminal fragments**

Primary cortical neurons cultured in 6-well plates for 7-10 DIV were treated with either HSA or AGE-HSA, in the presence or absence of anti-RAGE antibody (H300), Cathepsin B inhibitor (Calbiochem, #205531) and BACE 1 inhibitor (AZD3293) washed twice with cold PBS, and lysed in RIPA buffer, centrifuged, and protein was quantified. Proteins were resolved by 10% Tris-glycine SDS-PAGE for

APP695 and by 16.5% Tris-tricine SDS-PAGE for APP C-terminal fragments (CTFs).[36] Following SDS-PAGE, proteins were transferred onto 0.2 μm PVDF membrane. Western blotting for APP695 and APP CTFs (raised against 20 C-terminal amino acids of APP695) was performed using Y188 antibody (1:2000). Western blotting for beta tubulin was performed using beta tubulin primary monoclonal antibody (1:5000) and HRP-conjugated goat anti-mouse IgG secondary antibody (1:2500). APP695, APP-CTFs and beta tubulin were detected using ECL prime advance system, as per the manufacturer's instructions.

**Plasmids**

Three plasmids were used to assess the APP processing by the luciferase reporter assay. Full length APP cloned in pRC-CMV-APP695-Gal4 was used as described earlier.[36] Briefly, it is a pRC-CMV vector encoding a human APP695 fused in-frame at its C-terminus to the yeast transcription factor Gal4 via a glycine hinge. pFR-Luciferase reporter vector with firefly (*Photinus pyralis*) luciferase gene under the control of a synthetic promoter containing 5 tandem repeats of the yeast Gal4 activation sequence upstream of a minimal TATA box was used. A phRL-thymidine kinase (TK) vector containing sea pansy (*Renilla reniformis*) luciferase gene under control of the herpes simplex virus-TK promoter was the third vector co-transfected. The latter two plasmids were procured from promega.

**Dual-Glo luciferase gene reporter assay**

pRC-APP695-Gal4 and pFR-Luciferase (0.5 μg) were transfected into primary cortical neurons cultured in 24-well plates at 5 DIV, using Lipofectamine 2000 (1 μL/well). All wells were co-transfected with phRL-TK-Renilla (0.5 μg) as an internal control for luciferase expression. Transfection mixes containing lipid and DNA were prepared separately in OptiMEM I reduced serum medium (Gibco, #31985062), then mixed and incubated at RT for 25 min. After incubation, 75 μL/well transfection mix was added drop wise to the cells and incubated for 2 h. In one set of experiment, primary cortical neurons were pre-treated with γ-secretase inhibitor, N-[N-(3,5-difluorophenacetyl)-Lalanyl]-(S)-phenylglycine t-butyl ester for 30

min followed by transfection and treatment with HSA or AGE-HSA for 24 h (Figure 5A). In second set of experiment, primary cortical neurons were pre-treated with Cathepsin B inhibitor, CA074-Me or anti-RAGE antibody, H300 for 30 min followed by transfection and treatment with HSA or AGE-HSA for 8 h. Post treatment, quantification of firefly luciferase and renilla luciferase expression was measured (Figure 5B). Neurons were lysed with Glo-lysis buffer (50 µL/well) (Promega, #E2661), and the Dual-Glo luciferase activity assay was performed according to the manufacturer's instructions (Promega, #E2940). Luciferase signals were captured using a microplate luminometer (Promega). Firefly luciferase reporters activity was normalized using the renilla luciferase activity, which helps to differentiate between specific and nonspecific cellular responses and control for transfection efficiencies across experiments.[35]

**Determination of $A\beta_{1-42}$ release**

To determine the effect of AGE-HSA on $A\beta_{1-42}$ release from primary cortical neurons, cells were grown in 6 well plates, the conditioned neuronal growth medium at 5 DIV was removed, and neurons were washed twice with warm (37°C) PBS, pH 7.4, to remove Aβ that had accumulated with time in culture. Then, 500 µl of fresh, warm (37°C) neurobasal medium without phenol red, supplemented with B-27, containing either HSA or glycated HSA; in the presence or absence of Cathepsin B inhibitor (CA074Me) or BACE 1 inhibitor (AZD3293) or Anti-RAGE antibody (H300) was added to the neurons for a further 24 h. The neurobasal medium (300 µl) was harvested and transferred to 1.5 ml tubes containing complete protease inhibitor cocktail and centrifuged at 10,000 × g for 30 min at 4°C. Samples (200 µl) were then added to a mouse $A\beta_{1-42}$ ELISA plate and processed for detection of $A\beta_{1-42}$ according to the manufacturer's instructions (Invitrogen, #KMB3441). $A\beta_{1-42}$ levels in conditioned medium were calculated from a mouse $A\beta_{1-42}$ standard curve.

**Human tissue samples**

Human brain tissue homogenates were provided by the London Neurodegenerative Brain Bank which is funded by grants from the UK Medical Research Council and by Brains for Dementia Research, a joint

venture between Alzheimer's Society and Alzheimer's Research UK.Brains for Dementia Research has ethics approval from London–City and East NRES committee 08/H0704/128+5 and all participants gave informed consent for their tissue to be used in research. Tissue samples from the temporal cortex were dissected from frozen brains of 3 AD cases (age 84.3 ± 6.3 years) and 3 age matched controls (age 89.3 ± 11.3 years) and were homogenised in RIPA buffer at King's College London, UK.

**Statistical analyses**

Statistical analyses were performed using either Student's t-test (two-group comparison) or one-way ANOVA. Unpaired t-test was used to study the differential expression of proteins in human brain tissue homogenates of Normal and AD subjects.

**SUPPORTING INFORMATION**

Table S1. List of glycated peptides identified by High resolution accurate mass spectrometry

Table S2. List of identified Proteins and peptides

Table S3. List of differentially regulated proteins upon AGE induction

Table S4. Functional annotation of GO Process by DAVID analysis

Supplemental methods and figures

**AUTHOR CONTRIBUTIONS**

M.J.K. conceived the idea, designed, supervised the study. M.J.K., K.B.B. and R.W. have written the manuscript. K.B.B. and R.G. carried out the neuro2a cell experiments and have carried out western blotting and proteomic analysis including protein extraction, digestions and mass spectrometric acquisitions. R.M.B. was involved in cytoscape analysis and apoptosis studies, R.W., K.B.B. and O.K. were involved in primary cell culture experiments and analysis. All authors reviewed the manuscript.

**ACKNOWLEDGEMENTS**

This work was supported by the CSIR (grant BSC0115), the British Council Newton Fund (228125816) and the Dunhill Medical Trust (R320/1113). The authors thank Brains for Dementia Research for supplying human brain tissue. K.B.B. acknowledges CSIR, DBT and The British Council for research fellowship support.

**CONFLICT OF INTEREST:** Authors declare no conflict of interest.

**ABBREVIATIONS**

**AD** Alzheimer's disease

**AEP** Asparagine Endopeptidase

**AGE** Advanced glycation end products

**Aβ** Amyloid beta

**APP** Amyloid precursor protein

**BACE1** Beta-secretase 1

**CML** Carboxymethyllysine

**CTF** C-terminal fragments

**β-CTF** C-terminal fragment of β-secretase cleavage

**DIV** Days in vitro

**DCF-DA** 2′,7′-Dichlorofluorescin diacetate

**GSK3β** Glycogen synthase kinase 3β

**HSA** Human serum albumin

**PP2A** Protein phosphatase 2A

**RAGE** Receptor for advanced glycation end products**SWATH** Sequential window acquisition of all theoretical fragment ion spectra

## REFERENCES

1. Prince, M., Bryce, R., Albanese, E., Wimo, A., Ribeiro, W., and Ferri, C. P. (2013) The global prevalence of dementia: a systematic review and metaanalysis, *Alzheimer's & Dementia 9*, 63-75. e62.

2. Grundke-Iqbal, I., Iqbal, K., Tung, Y.-C., Quinlan, M., Wisniewski, H. M., and Binder, L. I. (1986) Abnormal phosphorylation of the microtubule-associated protein tau (tau) in Alzheimer cytoskeletal pathology, *Proceedings of the National Academy of Sciences 83*, 4913-4917.

3. Ittner, L. M., and Götz, J. (2011) Amyloid-β and tau- a toxic pas de deux in Alzheimer's disease, *Nature Reviews Neuroscience 12*, 67-72.

4. Bishop, N. A., Lu, T., and Yankner, B. A. (2010) Neural mechanisms of ageing and cognitive decline, *Nature 464*, 529-535.

5. Nunomura, A., Perry, G., Aliev, G., Hirai, K., Takeda, A., Balraj, E. K., Jones, P. K., Ghanbari, H., Wataya, T., and Shimohama, S. (2001) Oxidative damage is the earliest event in Alzheimer disease, *Journal of Neuropathology & Experimental Neurology 60*, 759-767.

6. Smith, M. A., Hirai, K., Hsiao, K., Pappolla, M. A., Harris, P. L., Siedlak, S. L., Tabaton, M., and Perry, G. (1998) Amyloid□β Deposition in Alzheimer Transgenic Mice Is Associated with Oxidative Stress, *Journal of neurochemistry 70*, 2212-2215.

7. Vitek, M. P., Bhattacharya, K., Glendening, J. M., Stopa, E., Vlassara, H., Bucala, R., Manogue, K., and Cerami, A. (1994) Advanced glycation end products contribute to amyloidosis in Alzheimer disease, *Proceedings of the National Academy of Sciences 91*, 4766-4770.

8. Christen, Y. (2000) Oxidative stress and Alzheimer disease, *The American journal of clinical nutrition 71*, 621s-629s.

9. Kassaar, O., Morais, M. P., Xu, S., Adam, E. L., Chamberlain, R. C., Jenkins, B., James, T., Francis, P. T., Ward, S., and Williams, R. J. (2017) Macrophage Migration Inhibitory Factor is subjected to glucose modification and oxidation in Alzheimer's Disease, *Scientific Reports 7*.

10. Schrijvers, E. M., Witteman, J., Sijbrands, E., Hofman, A., Koudstaal, P. J., and Breteler, M. (2010) Insulin metabolism and the risk of Alzheimer disease The Rotterdam Study, *Neurology 75*, 1982-1987.

11. El Khoury, N. B., Gratuze, M., Papon, M. A., Bretteville, A., and Planel, E. (2014) Insulin dysfunction and Tau pathology, *Frontiers in cellular neuroscience 8*.

12. Kandimalla, R., Thirumala, V., and Reddy, P. H. (2016) Is Alzheimer's disease a Type 3 Diabetes? A critical appraisal, *Biochimica et Biophysica Acta (BBA)-Molecular Basis of Disease 1863*, 1078-1089.

13. Sajan, M., Hansen, B., Ivey, R., Sajan, J., Ari, C., Song, S., Braun, U., Leitges, M., Farese-Higgs, M., and Farese, R. V. (2016) Brain Insulin Signaling Is Increased in Insulin-Resistant States and Decreases in

FOXOs and PGC-1α and Increases in Aβ1–40/42 and Phospho-Tau May Abet Alzheimer Development, *Diabetes 65*, 1892-1903.

14. Brownlee, M., Michael. (1995) Advanced protein glycosylation in diabetes and aging, *Annual review of medicine 46*, 223-234.

15. Thornalley, P. J. (2003) Use of aminoguanidine (Pimagedine) to prevent the formation of advanced glycation endproducts, *Archives of biochemistry and biophysics 419*, 31-40.

16. Cai, W., Uribarri, J., Zhu, L., Chen, X., Swamy, S., Zhao, Z., Grosjean, F., Simonaro, C., Kuchel, G. A., and Schnaider-Beeri, M. (2014) Oral glycotoxins are a modifiable cause of dementia and the metabolic syndrome in mice and humans, *Proceedings of the National Academy of Sciences 111*, 4940-4945.

17. Li, X.-H., Lv, B.-L., Xie, J.-Z., Liu, J., Zhou, X.-W., and Wang, J.-Z. (2012) AGEs induce Alzheimer-like tau pathology and memory deficit via RAGE-mediated GSK-3 activation, *Neurobiology of aging 33*, 1400-1410.

18. Smith, M. A., Taneda, S., Richey, P. L., Miyata, S., Yan, S.-D., Stern, D., Sayre, L. M., Monnier, V. M., and Perry, G. (1994) Advanced Maillard reaction end products are associated with Alzheimer disease pathology, *Proceedings of the National Academy of Sciences 91*, 5710-5714.

19. Choi, B.-R., Cho, W.-H., Kim, J., Lee, H. J., Chung, C., Jeon, W. K., and Han, J.-S. (2014) Increased expression of the receptor for advanced glycation end products in neurons and astrocytes in a triple transgenic mouse model of Alzheimer's disease, *Experimental & molecular medicine 46*, e75.

20. Takuma, K., Fang, F., Zhang, W., Yan, S., Fukuzaki, E., Du, H., Sosunov, A., McKhann, G., Funatsu, Y., and Nakamichi, N. (2009) RAGE-mediated signaling contributes to intraneuronal transport of amyloid-β and neuronal dysfunction, *Proceedings of the National Academy of Sciences 106*, 20021-20026.

21. Li, X., Du, L., Cheng, X., Jiang, X., Zhang, Y., Lv, B., Liu, R., Wang, J., and Zhou, X. (2013) Glycation exacerbates the neuronal toxicity of β-amyloid, *Cell death & disease 4*, e673.

22. Deane, R., Singh, I., Sagare, A. P., Bell, R. D., Ross, N. T., LaRue, B., Love, R., Perry, S., Paquette, N., and Deane, R. J. (2012) A multimodal RAGE-specific inhibitor reduces amyloid β–mediated brain disorder in a mouse model of Alzheimer disease, *The Journal of clinical investigation 122*, 1377-1392.

23. Piras, S., Furfaro, A., Domenicotti, C., Traverso, N., Marinari, U. M., Pronzato, M. A., and Nitti, M. (2016) RAGE expression and ROS generation in neurons: differentiation versus damage, *Oxidative medicine and cellular longevity*.

24. Ahmed, N., Ahmed, U., Thornalley, P. J., Hager, K., Fleischer, G., and Münch, G. (2005) Protein glycation, oxidation and nitration adduct residues and free adducts of cerebrospinal fluid in Alzheimer's disease and link to cognitive impairment, *Journal of neurochemistry 92*, 255-263.

25. Bhonsle, H. S., Korwar, A. M., Kote, S. S., Golegaonkar, S. B., Chougale, A. D., Shaik, M. L., Dhande, N. L., Giri, A. P., Shelgikar, K. M., and Boppana, R. (2012) Low plasma albumin levels are associated with increased plasma protein glycation and HbA1c in diabetes, *Journal of proteome research 11*, 1391-1396.

26. Wautier, M.-P., Chappey, O., Corda, S., Stern, D. M., Schmidt, A. M., and Wautier, J.-L. (2001) Activation of NADPH oxidase by AGE links oxidant stress to altered gene expression via RAGE, *American Journal of Physiology-Endocrinology And Metabolism 280*, E685-E694.

27. Yan, S. D., Schmidt, A. M., Anderson, G. M., Zhang, J., Brett, J., Zou, Y. S., Pinsky, D., and Stern, D. (1994) Enhanced cellular oxidant stress by the interaction of advanced glycation end products with their receptors/binding proteins, *Journal of Biological Chemistry 269*, 9889-9897.

28. Basurto-Islas, G., Grundke-Iqbal, I., Tung, Y. C., Liu, F., and Iqbal, K. (2013) Activation of asparaginyl endopeptidase leads to Tau hyperphosphorylation in Alzheimer disease, *Journal of Biological Chemistry 288*, 17495-17507.

29. Hook, V. Y., and Reisine, T. D. (2003) Cysteine proteases are the major β□secretase in the regulated secretory pathway that provides most of the β□amyloid in Alzheimer's disease: Role of BACE 1 in the constitutive secretory pathway, *Journal of neuroscience research 74*, 393-405.

30. Kominami, E., Ueno, T., Muno, D., and Katunuma, N. (1991) The selective role of cathepsins B and D in the lysosomal degradation of endogenous and exogenous proteins, *FEBS letters 287*, 189-192.

31. Hook, V. Y., Kindy, M., and Hook, G. (2008) Inhibitors of cathepsin B improve memory and reduce β-amyloid in transgenic Alzheimer disease mice expressing the wild-type, but not the Swedish mutant, β-secretase site of the amyloid precursor protein, *Journal of Biological Chemistry 283*, 7745-7753.

32. Hook, V. Y., Kindy, M., Reinheckel, T., Peters, C., and Hook, G. (2009) Genetic cathepsin B deficiency reduces β-amyloid in transgenic mice expressing human wild-type amyloid precursor protein, *Biochemical and biophysical research communications 386*, 284-288.

33. Kindy, M. S., Yu, J., Zhu, H., El-Amouri, S. S., Hook, V., and Hook, G. R. (2012) Deletion of the cathepsin B gene improves memory deficits in a transgenic Alzheimer's disease mouse model expressing AβPP containing the wild-type β-secretase site sequence, *Journal of Alzheimer's Disease 29*, 827-840.

34. Guglielmotto, M., Aragno, M., Tamagno, E., Vercellinatto, I., Visentin, S., Medana, C., Catalano, M. G., Smith, M. A., Perry, G., and Danni, O. (2012) AGEs/RAGE complex upregulates BACE1 via NF-κB pathway activation, *Neurobiology of aging 33*, 196. e113-196. e127.

35. Law, B. M., Guest, A. L., Pullen, M. W., Perkinton, M. S., and Williams, R. J. (2017) Increased Foxo3a Nuclear Translocation and Activity is an Early Neuronal Response to β γ-Secretase-Mediated Processing of the Amyloid-β Protein Precursor: Utility of an APP-GAL4 Reporter Assay, *Journal of Alzheimer's Disease*, 1-16.

36. Hoey, S. E., Williams, R. J., and Perkinton, M. S. (2009) Synaptic NMDA receptor activation stimulates α-secretase amyloid precursor protein processing and inhibits amyloid-β production, *Journal of Neuroscience 29*, 4442-4460.

37. Arnaud, L., Chen, S., Liu, F., Li, B., Khatoon, S., Grundke-Iqbal, I., and Iqbal, K. (2011) Mechanism of inhibition of PP2A activity and abnormal hyperphosphorylation of tau by I 2 PP2A/SET, *FEBS letters 585*, 2653-2659.

38. Batkulwar, K. B., Bansode, S. B., Patil, G. V., Godbole, R. K., Kazi, R. S., Chinnathambi, S., Shanmugam, D., and Kulkarni, M. J. (2015) Investigation of phosphoproteome in RAGE signaling, *Proteomics 15*, 245-259.

39. Reddy, S., Bichler, J., Wells-Knecht, K. J., Thorpe, S. R., and Baynes, J. W. (1995) N epsilon-(carboxymethyl) lysine is a dominant advanced glycation end product (AGE) antigen in tissue proteins, *Biochemistry 34*, 10872-10878.

40. Röcken, C., Kientsch-Engel, R., Mansfeld, S., Stix, B., Stubenrauch, K., Weigle, B., Bühling, F., Schwan, M., and Saeger, W. (2003) Advanced glycation end products and receptor for advanced glycation end products in AA amyloidosis, *The American journal of pathology 162*, 1213-1220.

41. Ramasamy, R., Vannucci, S. J., Du Yan, S. S., Herold, K., Yan, S. F., and Schmidt, A. M. (2005) Advanced glycation end products and RAGE: a common thread in aging, diabetes, neurodegeneration, and inflammation, *Glycobiology 15*, 16R-28R.

42. Bansode, S. B., Chougale, A. D., Joshi, R. S., Giri, A. P., Bodhankar, S. L., Harsulkar, A. M., and Kulkarni, M. J. (2013) Proteomic analysis of protease resistant proteins in the diabetic rat kidney, *Molecular & Cellular Proteomics 12*, 228-236.

43. Vernace, V. A., Schmidt□Glenewinkel, T., and Figueiredo□Pereira, M. E. (2007) Aging and regulated protein degradation: who has the UPPer hand?, *Aging cell 6*, 599-606.

44. Lubitz, I., Ricny, J., Atrakchi□Baranes, D., Shemesh, C., Kravitz, E., Liraz□Zaltsman, S., Maksin□Matveev, A., Cooper, I., Leibowitz, A., and Uribarri, J. (2016) High dietary advanced glycation end products are associated with poorer spatial learning and accelerated Aβ deposition in an Alzheimer mouse model, *Aging cell 15*, 309-316.

45. Ramasamy, R., Vannucci, S. J., Yan, S. S. D., Herold, K., Yan, S. F., and Schmidt, A. M. (2005) Advanced glycation end products and RAGE: a common thread in aging, diabetes, neurodegeneration, and inflammation, *Glycobiology 15*, 16R-28R.

46. Li, J., and Schmidt, A. M. (1997) Characterization and functional analysis of the promoter of RAGE, the receptor for advanced glycation end products, *Journal of Biological Chemistry 272*, 16498-16506.

47. Huang, W. J., Zhang, X., and Chen, W. W. (2016) Role of oxidative stress in Alzheimer's disease, *Biomedical reports 4*, 519-522.

48. Bierhaus, A., Schiekofer, S., Schwaninger, M., Andrassy, M., Humpert, P. M., Chen, J., Hong, M., Luther, T., Henle, T., and Klöting, I. (2001) Diabetes-associated sustained activation of the transcription factor nuclear factor-κB, *Diabetes 50*, 2792-2808.

49. Smith, M. A., Sayre, L. M., Monnier, V. M., and Perry, G. (1995) Radical AGEing in Alzheimer's disease, *Trends in neurosciences 18*, 172-176.

50. Sundelöf, J., Sundström, J., Hansson, O., Eriksdotter-Jönhagen, M., Giedraitis, V., Larsson, A., Degerman-Gunnarsson, M., Ingelsson, M., Minthon, L., and Blennow, K. (2010) Higher cathepsin B levels in plasma in Alzheimer's disease compared to healthy controls, *Journal of Alzheimer's Disease 22*, 1223-1230.

51. Iqbal, K., Alonso, A. d. C., Chen, S., Chohan, M. O., El-Akkad, E., Gong, C.-X., Khatoon, S., Li, B., Liu, F., and Rahman, A. (2005) Tau pathology in Alzheimer disease and other tauopathies, *Biochimica et Biophysica Acta (BBA)-Molecular Basis of Disease 1739*, 198-210.

52. Hu, M., Waring, J. F., Gopalakrishnan, M., and Li, J. (2008) Role of GSK□3β activation and α7 nAChRs in Aβ1–42□induced tau phosphorylation in PC12 cells, *Journal of neurochemistry 106*, 1371-1377.

53. Iqbal, K., Liu, F., Gong, C.-X., Alonso, A. d. C., and Grundke-Iqbal, I. (2009) Mechanisms of tau-induced neurodegeneration, *Acta neuropathologica 118*, 53-69.

54. Planel, E., Miyasaka, T., Launey, T., Chui, D.-H., Tanemura, K., Sato, S., Murayama, O., Ishiguro, K., Tatebayashi, Y., and Takashima, A. (2004) Alterations in glucose metabolism induce hypothermia leading to tau hyperphosphorylation through differential inhibition of kinase and phosphatase activities: implications for Alzheimer's disease, *Journal of Neuroscience 24*, 2401-2411.

55. Li, X.-H., Xie, J.-Z., Jiang, X., Lv, B.-L., Cheng, X.-S., Du, L.-L., Zhang, J.-Y., Wang, J.-Z., and Zhou, X.-W. (2012) Methylglyoxal induces tau hyperphosphorylation via promoting AGEs formation, *Neuromolecular medicine 14*, 338-348.

56. Zhang, Z., Song, M., Liu, X., Kang, S. S., Kwon, I.-S., Duong, D. M., Seyfried, N. T., Hu, W. T., Liu, Z., and Wang, J.-Z. (2014) Cleavage of tau by asparagine endopeptidase mediates the neurofibrillary pathology in Alzheimer's disease, *Nature medicine 20*, 1254-1262.

57. Mao, A. J., Bechberger, J., Lidington, D., Galipeau, J., Laird, D. W., and Naus, C. C. (2000) Neuronal differentiation and growth control of neuro-2a cells after retroviral gene delivery of connexin43, *Journal of Biological Chemistry 275*, 34407-34414.

58. Cox, C. J., Choudhry, F., Peacey, E., Perkinton, M. S., Richardson, J. C., Howlett, D. R., Lichtenthaler, S. F., Francis, P. T., and Williams, R. J. (2015) Dietary (−)-epicatechin as a potent inhibitor of βγ-secretase amyloid precursor protein processing, *Neurobiology of aging 36*, 178-187.

59. Wang, Y. P., Wang, Z. F., Zhang, Y. C., Qing, T., and Wang, J. Z. (2004) Effect of amyloid peptides on serum withdrawal-induced cell differentiation and cell viability, *Cell research 14*, 467-472.

60. Barzegar, A., and Moosavi-Movahedi, A. A. (2011) Intracellular ROS protection efficiency and free radical-scavenging activity of curcumin, *PLoS One 6*, e26012.

61. LeBel, C. P., Ischiropoulos, H., and Bondy, S. C. (1992) Evaluation of the probe 2′, 7′-dichlorofluorescin as an indicator of reactive oxygen species formation and oxidative stress, *Chemical research in toxicology 5*, 227-231.

62. van Engeland, M., Ramaekers, F. C., Schutte, B., and Reutelingsperger, C. P. (1996) A novel assay to measure loss of plasma membrane asymmetry during apoptosis of adherent cells in culture, *Cytometry 24*, 131-139.

63. Vermes, I., Haanen, C., Steffens-Nakken, H., and Reutellingsperger, C. (1995) A novel assay for apoptosis flow cytometric detection of phosphatidylserine expression on early apoptotic cells using fluorescein labelled annexin V, *Journal of immunological methods 184*, 39-51.

64. Korwar, A. M., Vannuruswamy, G., Jagadeeshaprasad, M. G., Jayaramaiah, R. H., Bhat, S., Regin, B. S., Ramaswamy, S., Giri, A. P., Mohan, V., and Balasubramanyam, M. (2015) Development of diagnostic fragment ion library for glycated peptides of human serum albumin: targeted quantification in prediabetic, diabetic, and microalbuminuria plasma by parallel reaction monitoring, SWATH, and MSE, *Molecular & Cellular Proteomics 14*, 2150-2159.

65. Kazi, R. S., Banarjee, R. M., Deshmukh, A. B., Patil, G. V., Jagadeeshaprasad, M. G., and Kulkarni, M. J. (2017) Glycation inhibitors extend yeast chronological lifespan by reducing advanced glycation end products and by back regulation of proteins involved in mitochondrial respiration, *Journal of Proteomics 156*, 104-112.

66. Croft, N. P., de Verteuil, D. A., Smith, S. A., Wong, Y. C., Schittenhelm, R. B., Tscharke, D. C., and Purcell, A. W. (2015) Simultaneous quantification of viral antigen expression kinetics using data-independent (DIA) mass spectrometry, *Molecular & Cellular Proteomics 14*, 1361-1372.

67. Dennis, G., Sherman, B. T., Hosack, D. A., Yang, J., Gao, W., Lane, H. C., and Lempicki, R. A. (2003) DAVID: database for annotation, visualization, and integrated discovery, *Genome biology 4*, R60.

68. Verfaillie, A., Imrichová, H., Van de Sande, B., Standaert, L., Christiaens, V., Hulselmans, G., Herten, K., Sanchez, M. N., Potier, D., and Svetlichnyy, D. (2014) iRegulon: from a gene list to a gene regulatory network using large motif and track collections, *PLoS computational biology 10*, e1003731.

69. Morris, J. H., Apeltsin, L., Newman, A. M., Baumbach, J., Wittkop, T., Su, G., Bader, G. D., and Ferrin, T. E. (2011) clusterMaker: a multi-algorithm clustering plugin for Cytoscape, *BMC bioinformatics 12*, 436.

## FIGURE LEGENDS

**Figure 1: Effect of AGEs on the viability of neuro2a cells *in vitro*.** Neuro2a cells were treated with different concentrations of HSA or AGE-HSA (0.1, 0.5, 1.0 and 1.5 mg/ml) for 24 h. The effect of AGEs on the viability of cells was analyzed by MTT assay. One-way ANOVA was used to calculate the variances in HSA and AGE-HSA treated groups.

**Figure 2: Measurement of AGE-HSA induced ROS production and apoptosis in neuro2a cells.** (A) ROS generation after HSA or AGE-HSA stimulation was measured in neuronal cells using H2DCF-DA after administration of 1 h. $H_2$DCF-DA only treated cells served as control and fold change is presented relative to control measured by spectrofluorometer. (B) Neuro2a cells were treated with control, HSA, or AGE-HSA for 1 h, and DCF-DA fluorescence images were obtained at 30 min after treatment (Upper panel depicts the bright field images while lower panel shows the green field images). Flow cytometric analysis of neuro2a cells treated with (C) HSA or (D) AGE-HSA using Annexin V-FITC Apoptosis Detection Kit. (E) Bar graph depicting the percentage of apoptotic cells upon HSA or AGE-HSA stimulation. FITC, fluorescein isothiocyanate; PI, propidium iodide; BF, bright field; GF, green field. Student's t-test was used to compare ROS generation after HSA and AGE treatments.

**Figure 3: AGE-HSA regulates the expression of several proteins associated with different metabolic function in neuronal cells.** Pathway analysis of (A) up regulated and (B) down regulated proteins upon AGE-HSA stimulation by DAVID. Potential transcription factors co-regulating (C) up regulated and (D) down regulated proteins predicted using cytoscapeplugin, iRegulon. (E) Protein-protein interactions between deregulated proteins were analysed by using String and closely interacting proteins were identified using MCL algorithm of Clustermaker2 plugin in Cytoscape. (F) Bar graph demonstrating the fold change in the expression of key proteins implicated in AD. (Pathways represented in bar graph are with $P<0.05$)

**Figure 4: Western blot analysis of Cathepsin B and AEP in neuro2a cells and primary cortical neurons.** The levels of Cathepsin B and AEP expressed were measured in neuro2a cells (shown in A, B

and C) and in primary cortical neurons (shown in D, E and F) after HSA or AGE stimulation. A beta-tubulin was used to normalize the possible loading errors. (A) Western blot analysis of Cathepsin B and AEP expressed in the neuro2a cells after AGE stimulation for 24 hours. (B) Quantitative analysis of Cathepsin B levels detected with Western blot in neuro2a cells. The level of Cathepsin B protein expressed in control was set as 100%; levels of Cathepsin B expressed after 24 hours of HSA or AGE stimulation were calculated by comparing to that of control. Densitometric analysis showed a significant increase in Cathepsin B levels after AGE stimulation. (C) Quantitative analysis of AEP levels detected with Western blot in neuro2a cells. The level of AEP protein expressed in control was set as 100%; levels of AEP expressed after HSA or AGE stimulation were calculated by comparing to that of control. Densitometric analysis showed a significant increase in AEP levels after AGE stimulation. (D) Western blot analysis of Cathepsin B and AEP expressed in the primary cortical neurons after AGE stimulation for 24 hours. (E) Quantitative analysis of Cathepsin B levels detected with Western blot in primary cortical neurons. The level of Cathepsin B protein expressed in control was set as 100%; levels of Cathepsin B expressed after 24 hours of HSA or AGE or H300/AGE stimulation were calculated by comparing to that of control. Densitometric analysis showed a significant increase in Cathepsin B levels after AGE stimulation and blocking RAGE with an anti-RAGE antibody (H300) abolished AGE-induced Cathepsin B expression. (F) Quantitative analysis of AEP levels detected with Western blot in primary cortical neurons. The level of AEP protein expressed in control was set as 100%; levels of AEP expressed after HSA or AGE or H300/AGE stimulation were calculated by comparing to that of control. Densitometric analysis showed a significant increase in AEP levels after AGE stimulation and blocking RAGE with an anti-RAGE antibody (H300) abolished AGE-induced AEP expression. One-way ANOVA was used to compare the expression of Cathepsin B and AEP across treatments in neuro2a cells and primary cortical neurons.

**Figure 5: AGE stimulation increases Cathepsin B-dependent amyloidogenic APP processing in primary cortical neurons through RAGE.** (A) Primary cortical neurons were transfected with plasmid

encoding pFR-Luc firefly luciferase reporter gene and APP695-Gal4. All cells were co-transfected with phRL-TK plasmid that constitutively expresses Renilla luciferase. Dual-Glo luciferase activity assays were performed 24 h after HSA or AGE-HSA treatment for quantification of firefly and Renilla luciferase expression. Firefly luciferase activity was normalized using the Renilla luciferase activity. Cells were treated with 10 μM N-[N-(3,5-Diflurophenaacetyl-L-alanyl)]-S-phenylglycine t-Butyl Ester for 30 min before transfection. The assay result shows the increased expression of pFR-Luc firefly luciferase upon AGE stimulation. (B) Primary cortical neurons were treated with 5 μM CA074-Me or4 μg/ml H300 for 30 min before co-transfection with pFR-Luc firefly luciferase reporter gene, APP695-Gal4 and phRL-TK plasmids. Dual-Glo luciferase activity assay was performed 8 h after HSA or AGE-HSA stimulation for quantification of firefly and Renilla luciferase expression. Firefly luciferase activity was normalized using the Renilla luciferase activity. The assay result shows that pre-treatment of CA074-Me orH300 blocked the AGE induced expression of pFR-Luc firefly luciferase.(C) Western blot show the effect of HSA, AGE-HSA, CA074Me, H300 or AZD3293 (BACE1 inhibitor) on APP-CTFs formation. (D) ELISA result show the elevated release of $A\beta_{1-42}$ from primary cortical neurons after AGE-HSA stimulation which was decreased with pre-treatment of CA074-Me, H300 and AZD3293.*P<0.05, **P<0.005, ***P<0.0005, ****P<0.00005. One-way ANOVA was used to compare the $A\beta_{1-42}$ formation across control and treatment groups.

**Figure 6: Western blot analysis of phosphorylated and total tau in primary cultured cortical neurons.** The levels of tau and pTau were measured in primary cortical neurons (shown in A, B and C) after HSA or AGE-HSA or H300/AGE stimulation. A beta-tubulin was used to normalize the possible loading errors. (A) Western blot analysis of Tau and pTau after HSA or AGE or H300/AGE stimulation for 24 hours. (B) Quantitative analysis of Tau levels detected with Western blot in primary cortical neurons. The level of Tau protein expressed in control was set as 100%; levels of Tau expressed after 24 hours of HSA or AGE or H300/AGE stimulation were calculated by comparing to that of control. Densitometric analysis showed a no change in the expression of Tau levels after AGE stimulation. (C)

Quantitative analysis of pTau levels detected with Western blot in primary cortical neurons. The level of pTau protein in control was set as 100%; levels of pTau expressed after 24 hours of HSA or AGE or H300/AGE stimulation were calculated by comparing to that of control. Densitometric analysis showed a notable increase in pTau levels after AGE stimulation. One-way ANOVA was used to study the levels of Tau and pTau in control and treatment groups.

**Figure 7: Representative western blot analysis of brain tissue lysates from the temporal cortex of AD subjects compared with age matched controls.** (A) The levels of glycated proteins (CML modified), RAGE, Cathepsin B, AEP and pTau were measured in normal and AD subjects. Raw intensity values (without normalization) are plotted for the quantitative analysis of western blots. (B) Quantitative analysis of carboxymethylated protein levels detected with Western blot in Healthy and AD subjects. Densitometric analysis showed a notable increase in glycated protein levels in AD subjects. (C) Quantitative analysis of RAGE expression detected by Western blot in Healthy and AD subjects. Densitometric analysis showed elevated RAGE expression in AD subjects as compared to Normal. (D) Quantitative analysis of Cathepsin B protein levels detected by Western blot in Healthy and AD subjects. Densitometric analysis showed increased levels of Cathepsin B in AD subjects. (E) Quantitative analysis of AEP protein levels detected by Western blot in Healthy and AD subjects. Densitometric analysis showed elevated levels of AEP in AD subjects than healthy individuals. (F) Quantitative analysis of pTau levels detected by Western blot in Healthy and AD subjects. Densitometric analysis showed elevated levels of pTau in AD subjects than normal individuals. The unpaired t-test was used to study the differential expression of proteins in human brain tissue homogenates.

## TABLES AND FIGURES

**Table 1:** Levels of RAGE, Cathepsin B, AEP, pTau and CML modified proteins in Normal and AD subjects normalized with beta-tubulin.

Data is expressed as Mean ± SEM.

| Sr. No. | Protein Name | Ratio to β-tubulin | | *p* Value |
|---|---|---|---|---|
| | | Normal | AD | |
| 1 | CML | 0.72±0.39 | 11.75±3.99 | 0.0513 |
| 2 | RAGE | 0.35±0.22 | 4.73±1.3 | 0.0299 |
| 3 | Cathepsin B | 0.17±0.10 | 3.09±0.95 | 0.0388 |
| 4 | AEP | 0.18±0.08 | 3.35±1.22 | 0.0615 |
| 5 | pTau | 0.12±0.06 | 3.16±0.75 | 0.016 |

**Figure 1**

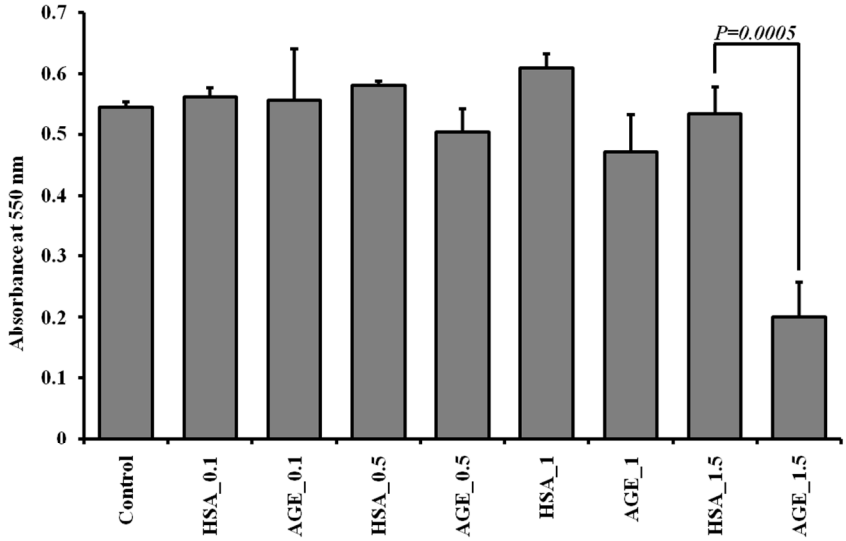


**Figure 2**

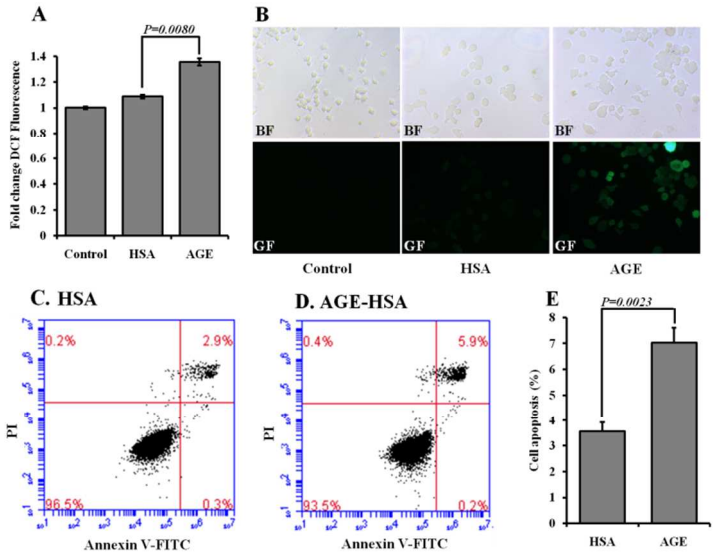

**Figure 3**

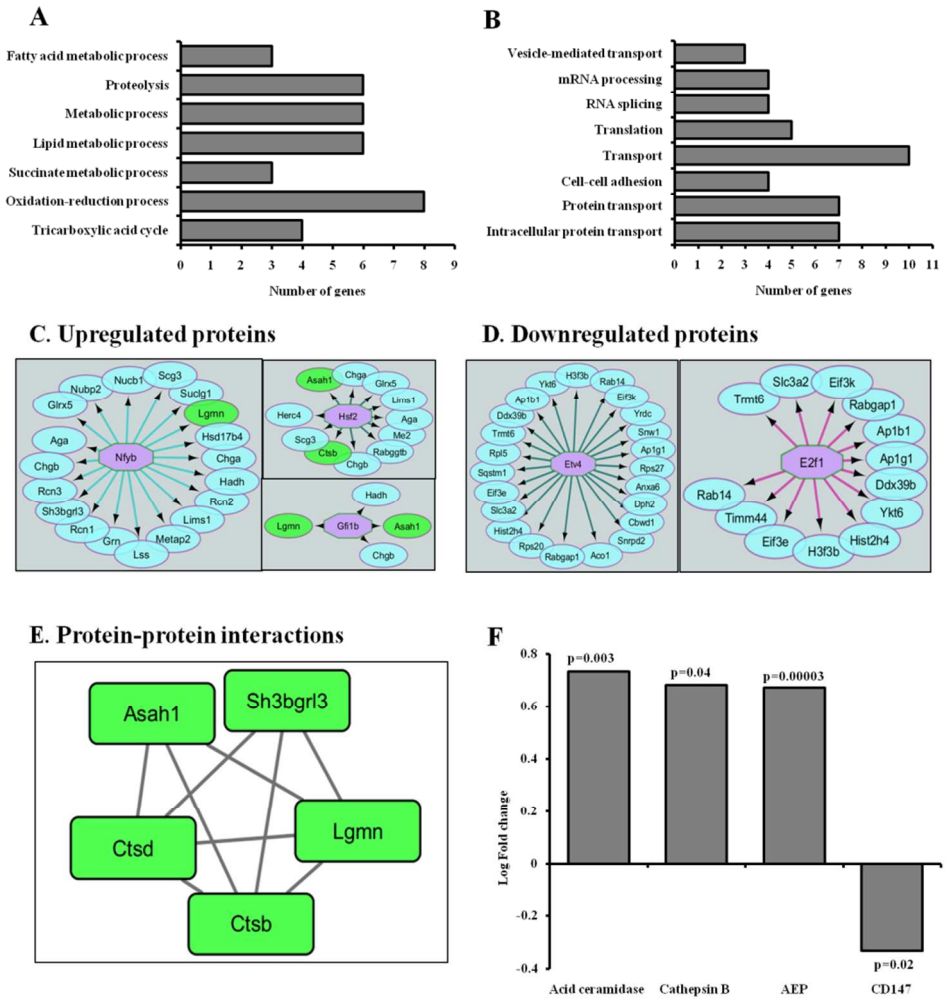
A
Fatty acid metabolic process
Proteolysis
Metabolic process
Lipid metabolic process
Succinate metabolic process
Oxidation-reduction process
Tricarboxylic acid cycle
0 1 2 3 4 5 6 7 8 9
Number of genes
B
Vesicle-mediated transport
mRNA processing
RNA splicing
Translation
Transport
Cell-cell adhesion
Protein transport
Intracellular protein transport
0 1 2 3 4 5 6 7 8 9 10 11
Number of genes
C. Upregulated proteins
D. Downregulated proteins
E. Protein-protein interactions
Asah1
Sh3bgrl3
Ctsd
Lgmn
Ctsb
F
p=0.003
p=0.04
p=0.00003
p=0.02
Log Fold change
0.8
0.6
0.4
0.2
0
-0.2
-0.4
Acid ceramidase
Cathepsin B
AEP
CD147

**Figure 4**

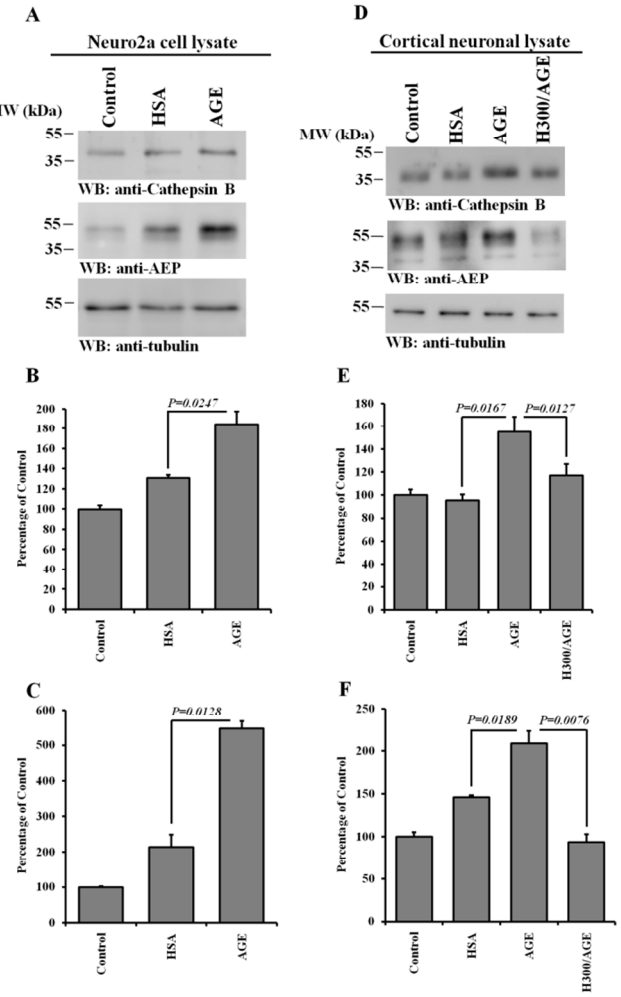


**Figure 5**

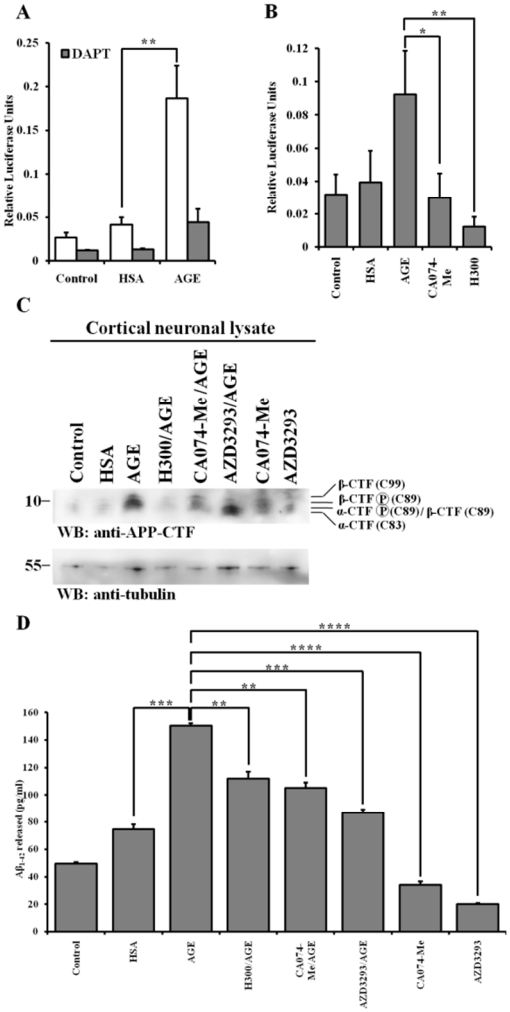

**Figure 6**

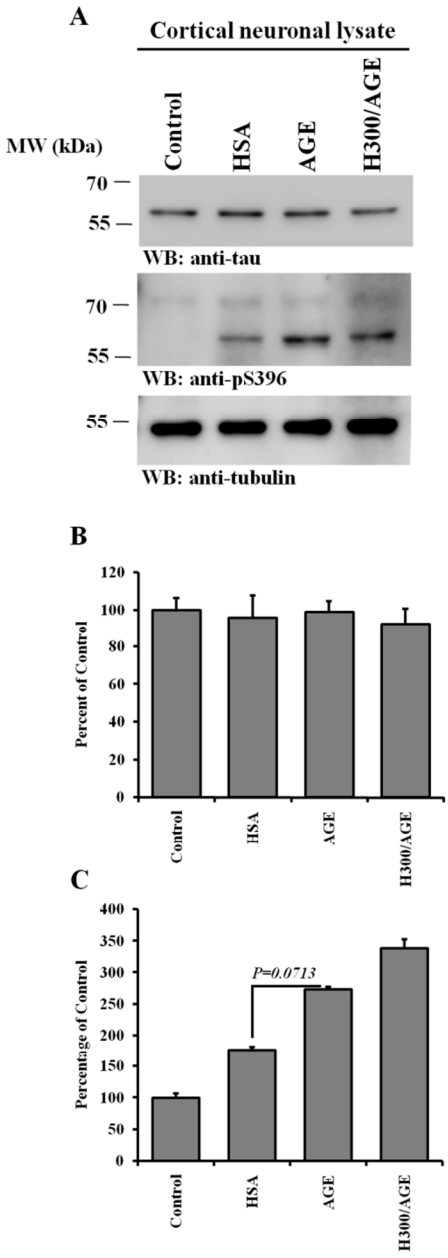


**Figure 7**

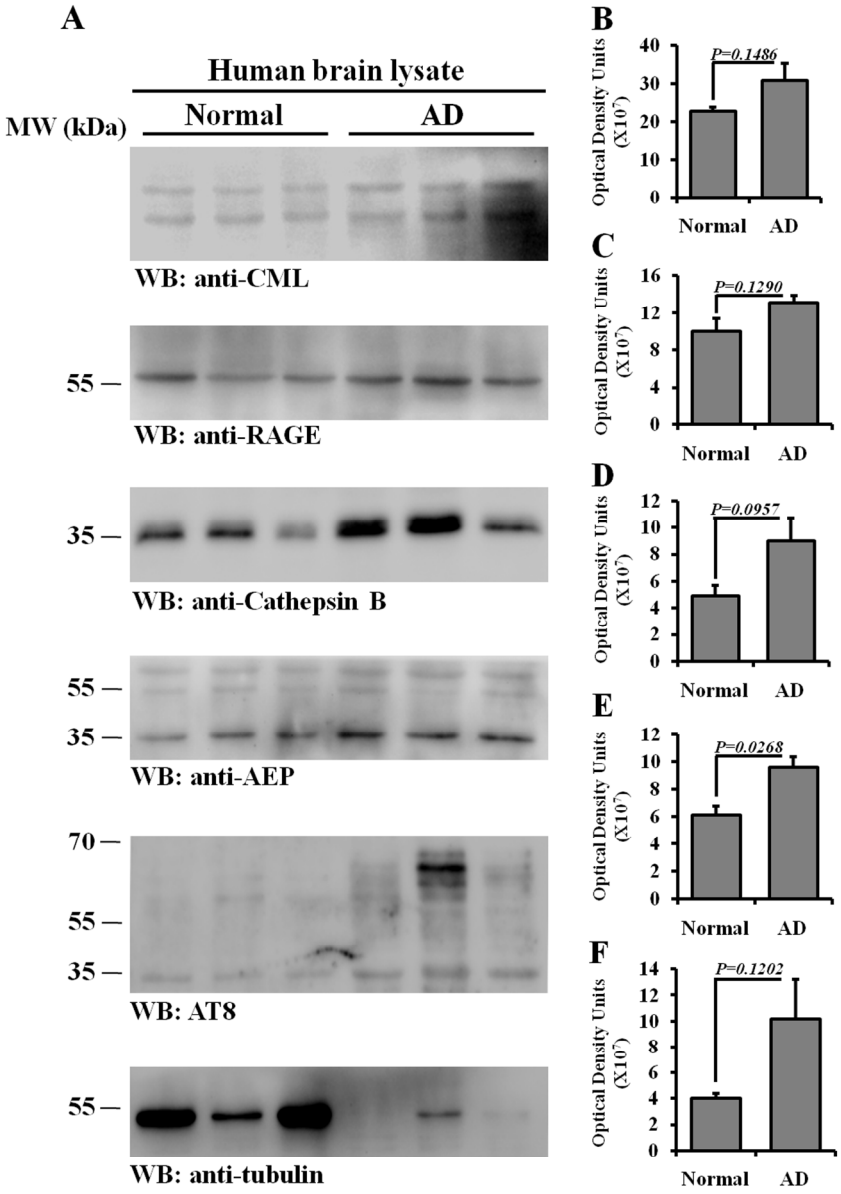

**For Table of Contents Use Only**

# Advanced glycation end products modulate amyloidogenic APP processing and Tau phosphorylation: a mechanistic link between glycation and the development of Alzheimer's disease

Kedar Batkulwar, Rashmi Godbole, Reema Banarjee, Omar Kassaar, Robert J Williams, Mahesh J Kulkarni

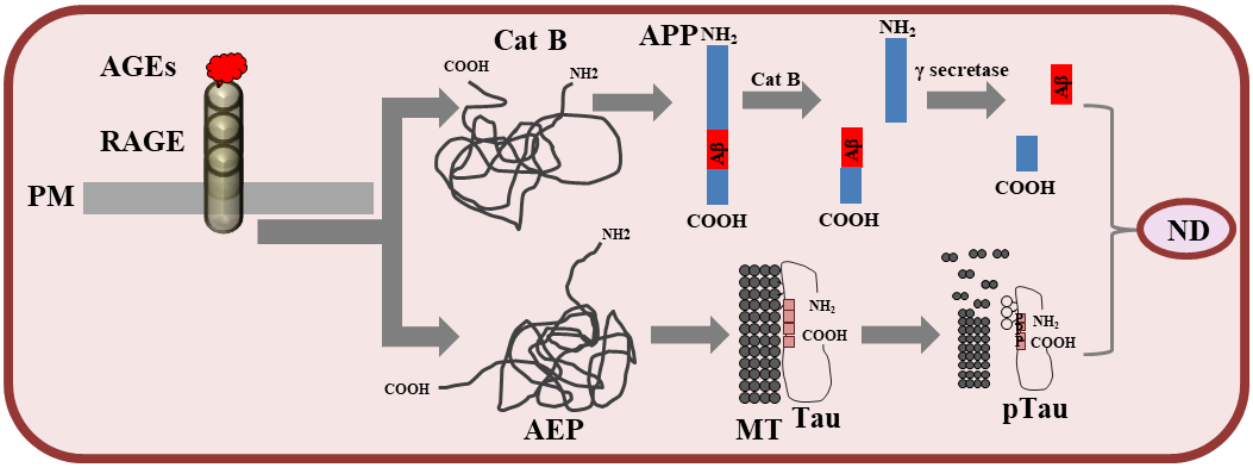


**TOC Graphic:** AGEs induce the expression of Cathepsin B and AEP causing increased Aβ formation and Tau phosphorylation respectively resulting in neuronal damage. (PM-Plasma membrane, Cat B-Cathepsin B, APP-Amyloid precursor protein, AEP-Asparagine endopeptidase, MT-Microtubules pTau- Phosphorylated Tau and ND-Neurodegeneration).